Role of Nrf2 Signaling in the Regulation of Vascular BK Channel β1 Subunit Expression and BK Channel Function in High-Fat Diet–Induced Diabetic Mice

Tong Lu,[1] Xiaojing Sun,[1] Yong Li,[1,2] Qiang Chai,[3] Xiao-Li Wang,[1] and Hon-Chi Lee[1]

The large conductance Ca^{2+}-activated K^+ (BK) channel β1-subunit (BK-β1) is a key modulator of BK channel electrophysiology and the downregulation of BK-β1 protein expression in vascular smooth muscle cells (SMCs) underlies diabetic vascular dysfunction. In this study, we hypothesized that the nuclear factor erythroid-2–related factor 2 (Nrf2) signaling pathway plays a significant role in the regulation of coronary BK channel function and vasodilation in high-fat diet (HFD)–induced obese/diabetic mice. We found that the protein expressions of BK-β1 and Nrf2 were markedly downregulated, whereas those of the nuclear factor-κB (NF-κB) and the muscle ring finger protein 1 (MuRF1 [a ubiquitin E3 ligase for BK-β1]) were significantly upregulated in HFD mouse arteries. Adenoviral expression of Nrf2 suppressed the protein expressions of NF-κB and MuRF1 but enhanced BK-β1 mRNA and protein expressions in cultured coronary SMCs. Knockdown of Nrf2 resulted in reciprocal changes of these proteins. Patch-clamp studies showed that coronary BK-β1–mediated channel activation was diminished in HFD mice. Importantly, the activation of Nrf2 by dimethyl fumarate significantly reduced the body weight and blood glucose levels of HFD mice, enhanced BK-β1 transcription, and attenuated MuRF1-dependent BK-β1 protein degradation, which in turn restored coronary BK channel function and BK channel–mediated coronary vasodilation in HFD mice. Hence, Nrf2 is a novel regulator of BK channel function with therapeutic implications in diabetic vasculopathy.

Diabetes is closely associated with increased risks of cardiovascular diseases, which are the leading cause of death in the U.S. The large-conductance calcium-activated potassium (BK) channels are abundantly expressed in coronary arterial smooth muscle cells (SMCs), playing an important role in regulating coronary circulation and myocardial perfusion (1–4). Functional vascular BK channels are composed of the pore-forming α-subunits and the regulatory β1-subunits (BK-β1) in 4:4 stoichiometry. The BK-β1, encoded by the KCNMB1 gene, is a key determinant of BK channel electrophysiology. The presence of BK-β1 enhances BK channel α-subunit sensitivity to Ca^{2+}, allowing channel activation in the physiological range of Ca^{2+} concentrations and membrane potentials (5–7). Activation of BK channels hyperpolarizes the membrane potentials of vascular SMC, leading to the reduction of intracellular Ca^{2+} concentration and vascular relaxation. However, in response to increased oxidative stress, the vascular BK channel function is impaired, with reduced BK-β1 protein expression being a common feature in the vascular SMCs of prediabetic, type 1 diabetic, and type 2 diabetic animals (8–13).

The nuclear factor-κB (NF-κB) is a family of transcription factors that includes RelA (p65), RelB, c-Rel, and p105/p50 (NF-κB1) or p100/p52 (NF-κB2) subunits (14). Under baseline conditions, p65 is bound to an inhibitory NF-κB subunit (IκB) that keeps it sequestered in an inactive state in the cytoplasm of cells. Phosphorylation of IκB by IκB kinase promotes IκB degradation through the ubiquitin-proteasome system (UPS), which in turn releases p65 and facilitates the nuclear translocation of the p65/p50 or p65/p52 dimeric complex (14). In addition, the NF-κB/p65 can be directly activated by reactive oxygen species (ROS) through phosphorylation of NF-κB/p65 (15). We have recently identified that the muscle ring finger protein 1 (MuRF1), a muscle-specific E3 ligase, is one of the target

COMPLICATIONS

genes of NF-κB in vascular SMCs (16). An increase in the protein expressions of NF-κB/p50 and NF-κB/p65 was responsible for MuRF1-mediated BK-β1 protein degradation in type 1 diabetic mouse arteries (16). However, the upstream signaling leading to dysregulation of NF-κB expression in diabetic vessels is unclear.

The nuclear factor erythroid-2–related factor 2 (Nrf2) signaling plays a critical role in the maintenance of intracellular redox homeostasis by regulating multiple downstream antioxidant genes and phase II detoxification enzymes, which include NADPH dehydrogenase quinone 1, glutathione-disulfide reductase, glutathione translocase, thioredoxin, thioredoxin reductase 1, heme oxygenase-1 (HO-1), superoxide dismutase, catalase, and glutathione peroxidase (13,17–20). Activation of Nrf2 has been shown to be protective against hyperglycemia-induced, ROS-mediated apoptosis and cell damage in renal, cardiac, and vascular cells (21). C57BL/6 mice fed a high-fat diet (HFD) are an established diet-induced obese/diabetic mouse model (22–25) with metabolic features similar to those of human type 2 diabetes (9,25–27). In this study, we found that Nrf2 protein expression was significantly downregulated with an associated decrease of BK-β1 expression in vascular SMCs of HFD mice, resulting in coronary BK channelopathy and coronary vasculopathy. Pharmacological activation of Nrf2 not only suppressed the NF-κB/MuRF1-mediated protein degradation of BK-β1, but also augmented BK-β1 mRNA expression, protecting the BK channel function and BK channel–mediated coronary vasodilation in HFD mice. Hence, Nrf2 signaling represents a therapeutic target for cardiovascular complications in obesity and type 2 diabetes.

RESEARCH DESIGN AND METHODS

Animals and Diets
Male mice (C57BL/6J) at 4 weeks of age were purchased from The Jackson Laboratory. These animals were fed with a 60% fat diet (HFD) or 10% fat diet (low-fat diet [LFD]) for 6 months. In the dimethyl fumarate (DMF) treatment studies, after 6 months eating an HFD or LFD animals were randomly divided into four groups (DMF-treated LFD, placebo-treated LFD, DMF-treated HFD, and placebo-treated HFD) and were treated with DMF (25 mg/kg/daily) or placebo (same volume of vehicle) by gavage for 10 days (28,29). Tail blood pressures were measured using a CODA Non-Invasive Blood Pressure System (Kent Scientific Corporation, Torrington, CT), and blood glucose levels were determined using an Accu-CHEK Aviva Glucose Meter (Roche Diabetes Care Inc., Indianapolis, IN). All protocols were approved by the Institutional Animal Care and Use Committee of the Mayo Clinic (Rochester, MN).

Adenoviral Delivery of Nrf2 and Short Hairpin RNA
Human coronary arterial SMCs and the SmBM culture medium were purchased from Lonza Walkersville Inc. (Walkersville, MD). Cells between passages 5 and 8 were transduced with adenoviral green fluorescent protein (GFP) vectors carrying the Nrf2 gene (Ad-GFP-Nrf2) or Nrf2 short hairpin RNAs (shRNAs) (Ad-GFP-Nrf2 shRNA) at 50 multiplicity of infection (MOI) for 48 h as we previously described (11,16). Transduction of Ad-GFP or Ad-GFP-U6-Scramble-RNAi served as controls. All adenoviral vectors were obtained from Vector BioLabs (Malvern, PA).

Western Blot Analysis
Immunoblot analysis was performed in isolated arteries from mice and cultured coronary SMCs, as we reported previously (9,11,16). Rabbit anti-Nrf2 (1:200; catalog #sc-722; Santa Cruz Biotechnology), rabbit anti–HO-1 (1:200; catalog #sc-10789; Santa Cruz Biotechnology), and mouse anti-MuRF1 (1:200; catalog #sc-398608; Santa Cruz Biotechnology), mouse GAPDH-horseradish peroxidase (HRP) (1:5,000; catalog #HRP-6004; Proteintech), and mouse anti–β-actin-HRP (1:10,000; catalog #A3854; Sigma-Aldrich, St. Louis, MO) antibodies were used in this study. Rabbit anti–BK-β1 antibody (1:200) was custom made as previously reported (4). NF-κB family member antibody sample kit (1:200; catalog #4766S) was purchased from Cell Signaling Technology Inc. (Danvers, MA). Rabbit antiphospho-NF-κB p65 (Ser276) (1:200; catalog #PA5–37718) was obtained from ThermoFisher Scientific (Rockford, IL). The optical density of the bands was analyzed with Scion Image Software (Scion Corporation, Frederick, MD). Protein expression was expressed as relative abundance normalized to GAPDH or β-actin.

Mouse Coronary Arterial Myocytes Isolation and BK Current Recording
Single coronary SMC isolation and BK current recordings were performed as previously described (11,16). Whole-cell BK currents were defined as the iberiotoxin (IBTX; 100 nmol/L)-sensitive K^+ current component, and the inside-out single BK channel currents were determined by their unitary current amplitude and Ca^{2+} sensitivity, as previously described (30,31). For whole-cell BK channel recordings, the pipette solution contained the following (in mmol/L): KCl 140, $MgCl_2$ 0.5, Na_2ATP 5.0, Na_2GTP 0.5, HEPES 10.0, EGTA 1.0, $CaCl_2$ 0.465 (~200 nmol/L free Ca^{2+}) at pH 7.38. The bath solution contained the following (in mmol/L): NaCl 145.0, KCl 5.6, $MgCl_2$ 1.0, $CaCl_2$ 1.0, HEPES 10.0, and glucose 5.0 at pH 7.40. For inside-out single BK channel recordings, the pipette solution contained the following (in mmol/L): KCl 140.0, $CaCl_2$ 1.0, $MgCl_2$ 1.0, EGTA 1.0, and HEPES 10.0 at pH 7.4. The bath solution contained the following (in mmol/L): KCl 140.0, $MgCl_2$ 1.0, HEPES 10.0, EGTA 1.0, and $CaCl_2$ 0.465 at pH 7.38. Experiments were performed at room temperature (22°C).

Quantitative Real-time PCR
Isolation of total RNA, RT-PCR, and quantitative real-time PCR was performed as previously described (16). The reaction underwent a 40-cycle amplification with the following conditions: denaturalization for 15 s at 94°C; annealing for 30 s at 55°C; and extension for 30 s at 70°C. Copy numbers of the target gene were expressed as $2^{-\Delta Ct}$ (where

ΔCt = Ct of target gene − Ct of internal control gene, and Ct represents the threshold cycle). The forward and reverse primer sequences are listed as follows:

- Human BK-β1 forward: 5′-CTTCTCCGCACCTCGGGGGA-3′; reverse: 5′-CGGTCAGCAGGAAGGTGGGC-3′;
- Human GAPDH forward: 5′-ACCACAGTCCATGCCATC-ACTGCC-3′; reverse: 5′-ACCAGGAAATGAGCTTGACAAA-GT-3′;
- Mouse BK-β1 forward: 5′-TTCTGCACCTCAAGTCAACG-3′; reverse: 5′-TACTTCTGAGCCGCCAAGAT-3; and
- Mouse β-actin forward: 5′-TGTTACCAACTGGGACGACA-3′; reverse: 5′-CTGGGTCATCTTTTCACGGT-3′.

Videomicroscopy

Mouse coronary arteries (<100 μm in diameter) were dissected and vasoreactivity was measured as we have previously described (10,11). Only the vessels that showed no leak with 85% relaxation in response to 0.1 mmol/L nitroprusside and >35% constriction in response to 60 mmol/L KCl were used for experiments. BK channel–mediated coronary vasodilation was determined by the application of 100 nmol/L IBTX and subtracting the IBTX-insensitive component from total vasodilation.

Chemicals

Dehydrosoyasaponin-1 (DHS-1) was provided by Merck Research Laboratory (Boston, MA). Unless noted otherwise, all chemicals including DMF were purchased from Sigma-Aldrich. DMF was dissolved in DMSO and diluted with water into a 10 mmol/L stock solution.

Statistical Analysis

Data were expressed as the mean $\pm$ SEM. A Student t test was used to compare data between two groups. A paired t test was used to compare data before and after treatment. One-way ANOVA, followed by the Tukey test analysis was used to compare multiple groups using SigmaStat 3.5 software (Systat Software Inc., San Jose, CA). A statistically significant difference was defined as $P < 0.05$.

RESULTS

Metabolic Characterization of HFD Mice

After 6 months of HFD consumption, mice had significant increases in body weights, blood pressures, and random glucose and serum insulin levels, compared with those in control mice eating an LFD (Table 1).

Reduced BK-β1 Protein Expression With Impaired BK-β1 Function and BK Channel–Mediated Vasodilation in HFD Mice Was Associated With the Downregulation of Nrf2 Expression

We first compared the BK-β1 subunit–induced channel activation using a specific membrane-impermeable BK-β1 activator, DHS-1, in the excised membrane patches from freshly isolated coronary SMCs of LFD and HFD mice (Fig. 1A). The total BK single-channel open probability (nPo) was significantly decreased in HFD mice at baseline (0.09 $\pm$ 0.03, n = 23 cells) compared with that of LFD mice (0.33 $\pm$ 0.11, n = 23 cells, $P < 0.001$). Cytoplasmic application of 100 nmol/L DHS-1 robustly increased nPo to 0.68 $\pm$ 0.14 (n = 23 cells, $P < 0.001$ vs. baseline) in LFD mice. In contrast, the DHS-1 effects were modest though significant in HFD mice (0.17 $\pm$ 0.07, n = 23 cells, $P < 0.05$ vs. baseline, $P < 0.001$ vs. LFD with DHS-1).

Similar to streptozotocin-induced type 1 diabetic mice (16), HFD mice showed a significant reduction in BK-β1 protein expression by 57.1% (Fig. 1B), no change in BK-β1 mRNA expression (Fig. 1C), a 1.6-fold increase in MuRF1 protein expression, and a 51.8% reduction in Nrf2 protein expression in the arterial vessels of HFD mice compared with those of LFD mice (n = 6 mice for each group, $P < 0.05$) (Fig. 1B).

The BK channel–mediated coronary vasodilation was examined using NS-1619 (a BK channel activator) in LFD and HFD mice. As shown in Fig. 1D, NS-1619 dose-dependently dilated the coronary arteries of LFD mice with a half-maximal effective concentration of 0.09 $\pm$ 0.01 μmol/L and an efficacy of 71.72 $\pm$ 1.95% (n = 4 mice) but had reduced potency (half-maximal effective concentration 0.59 $\pm$ 0.06 μmol/L) and efficacy (19.16 $\pm$ 0.35%) in HFD mice (n = 4 mice, $P < 0.001$ vs. LFD for both). These results indicate that BK channel–mediated coronary vasodilation in HFD mice is impaired.
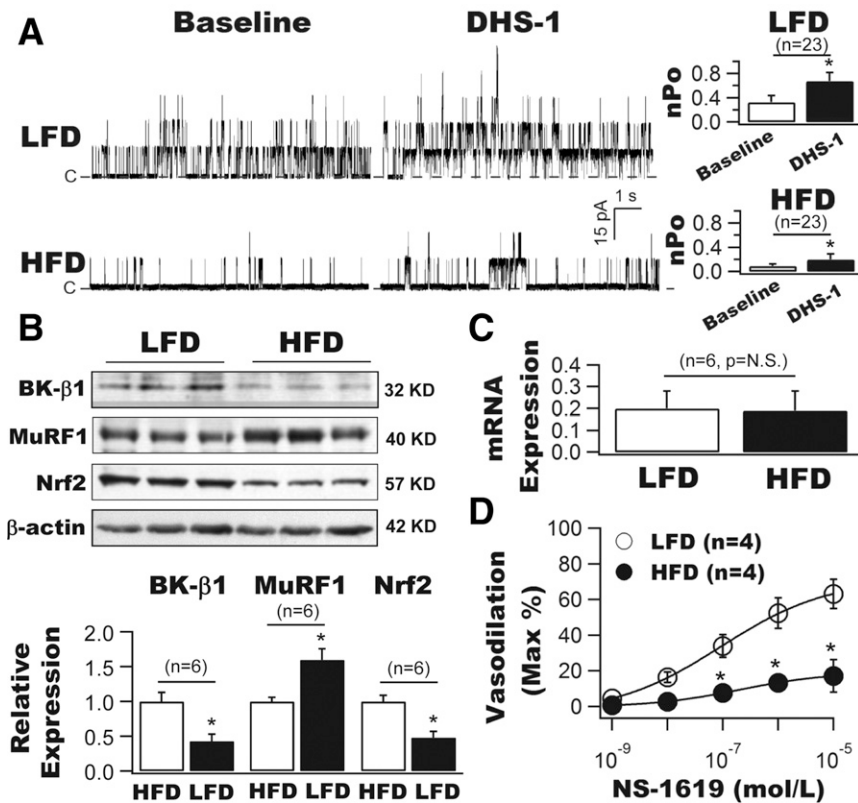
Regulation of HO-1, MuRF1, and BK-β1 Protein Expressions by Adenoviral Delivery of Nrf2 Gene in Cultured Coronary Arterial SMCs

We have identified that MuRF1 is an E3 ligase responsible for BK-β1 protein degradation in vascular SMCs (16). To further study the role of Nrf2 in the regulation of MuRF1-dependent BK-β1 protein expression, we manipulated the

Table 1—Metabolic characterization and blood pressure of mice (strain: C57BL/6J) 6 months after the consumption of a 10% fat diet (LFD) or a 60% fat diet (HFD)

Animal (n)	Body weight (g)	Glucose (mg/dL)	Insulin (ng/mL)	Systolic/diastolic pressure (mmHg)	Mean arterial pressure (mmHg)
LFD (n = 8–10)	30.4 $\pm$ 0.9	146.5 $\pm$ 12.6	0.97 $\pm$ 0.06	110.4 $\pm$ 4.4/82.6 $\pm$ 5.2	91.9 $\pm$ 4.8
HFD (n = 8–12)	48.1 $\pm$ 1.8	230.1 $\pm$ 9.7	6.64 $\pm$ 0.45	126.0 $\pm$ 3.5/94.8 $\pm$ 3.8	105.2 $\pm$ 3.7
P value	<0.05	<0.05	<0.05	<0.05	<0.05

There were significant increases in body weight, serum glucose level, serum insulin level, and mean blood pressure in HFD mice compared with LFD mice. Data are presented as mean $\pm$ SEM.

Figure 1—Downregulation of BK-β1 and Nrf2 protein expressions and upregulation of MuRF1 protein expressions in vascular SMCs are associated with coronary BK channel dysregulation and coronary arterial dysfunction in HFD mice. *A*: Inside-out single BK currents were recorded from freshly isolated coronary SMCs of LFD and HFD mice at baseline and after exposure to 100 nmol/L DHS-1 (a specific BK-β1 activator). The total channel nPo was significantly lower in HFD mice at baseline compared with LFD mice. DHS-1 robustly enhanced the channel activities, but the DHS-1 effects in HFD mice were diminished compared with those in LFD mice ($n = 23$ cells). Dashed lines indicate the closed state (C) of channels. *B*: BK-β1 protein expression was markedly downregulated and was accompanied by reduced Nrf2 expression and increased MuRF1 expression in the arterial vessels of HFD mice ($n = 6$ mice for each group). *C*: No difference in BK-β1 mRNA levels in coronary arteries from LFD and HFD mice ($n = 6$ mice for each group). *D*: Coronary vasodilation to NS-1619 (a BK channel activator) was impaired in HFD mice ($n = 4$ mice). *$P < 0.05$ vs. controls.

Nrf2 gene expression in cultured human coronary SMCs by adenoviral delivery (50 MOI) of the Nrf2 gene and Nrf2 shRNA. We found that a 6.8-fold increase in Nrf2 expression by Ad-Nrf2 transduction produced a 2.1-fold enhancement in HO-1 expression, a 66.2% reduction in MuRF1 expression, and a 2.3-fold argumentation in BK-β1 protein expression (Fig. 2*A*). In contrast, a 58.9% knockdown of Nrf2 expression by Ad-Nrf2 shRNA resulted in a 41.2% decrease in HO-1 expression, a 3.0-fold upregulation of MuRF1 expression, and a 68.9% downregulation of BK-β1 protein expression ($n = 9$ culture plates for all, $P < 0.05$ vs. controls) (Fig. 2*B*). These results indicate that MuRF1 and BK-β1 protein expressions are tightly regulated by the Nrf2 gene in coronary SMCs.

In addition, Ad-Nrf2 transduction significantly increased BK-β1 mRNA levels in cultured human and mouse coronary SMCs by 2.6-fold and 1.6-fold, respectively ($n = 9$ culture plates for both, $P < 0.05$ vs. Ad-GFP) (Fig. 2*C*), suggesting that the upregulation of BK-β1 protein expression by Nrf2 was also attributed to the enhanced mRNA transcription in vascular SMCs.

Regulation of NF-κB Protein Expression by Nrf2 in Coronary Arterial SMCs

Figure 3*A* illustrates the protein expressions of NF-κB subunits in the arteries of LFD and HFD mice. There was a 1.7-fold increase in NF-κB/p65 protein level ($n = 6$ mice, $P < 0.05$ vs. LFD) but no change in that of NF-κB/p50 ($n = 6$ mice, $P = $ NS vs. LFD) in HFD mice. To determine the effects of Nrf2 on NF-κB protein expression, we transduced Ad-Nrf2 in human coronary SMCs. After a 48-h transduction, the protein levels of NF-κB/p50, NF-κB/p65, and phospho-NF-κB/p65(S267) were reduced by 64.5%, 61.2%, and 58.0%, respectively ($n = 8$ culture plates) compared with cells transduced with Ad-GFP ($n = 7$ culture plates, $P < 0.05$). Hence, NF-κB protein expressions are profoundly regulated by Nrf2 in arterial SMCs.

Upregulation of Nrf2, HO-1, and BK-β1 Protein Expression and Downregulation of NF-κB and MuRF1 Expression in Cultured Coronary Arterial SMCs After Incubation With DMF

We examined the effects of DMF (a U.S. Food and Drug Administration–approved Nrf2 activator) on the protein
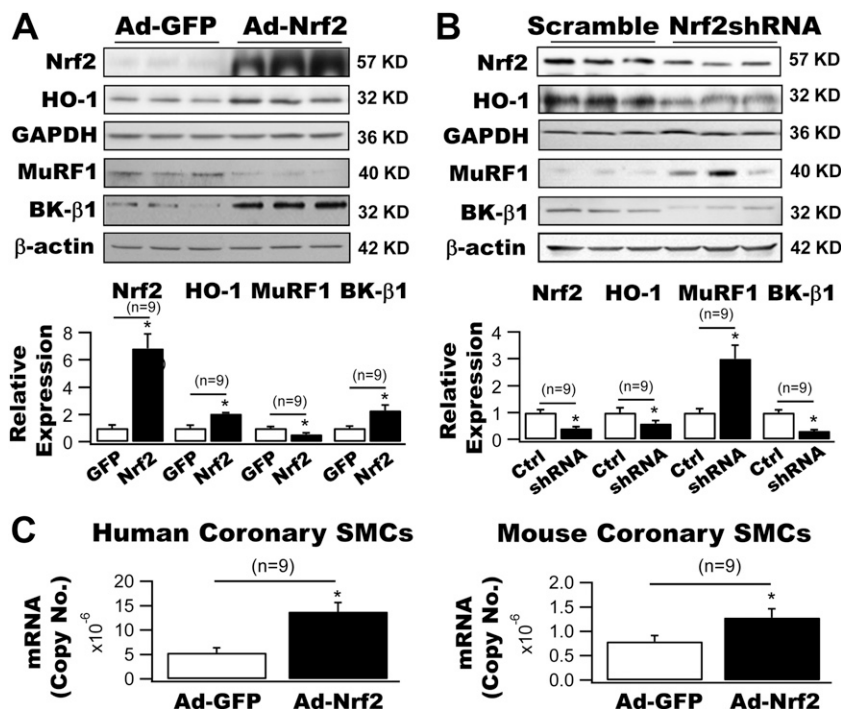
Figure 2—Regulation of HO-1, MuRF1, and BK-β1 expressions in cultured coronary SMCs by Nrf2. *A*: Ad-Nrf2 transduction (50 MOI) produced a 6.8-fold increase in Nrf2 expression and a 2.1-fold increase in HO-1 expression in human coronary SMCs. These changes were associated with a 66.2% reduction in MuRF1 expression and a 2.3-fold increase in BK-β1 expression (*n* = 9 culture plates). *B*: Transduction with Ad-Nrf2 shRNA (50 MOI) in human coronary arterial SMCs resulted in a 58.9% knockdown in the expression of Nrf2, a 41.2% reduction in that of HO-1, a threefold upregulation in that of MuRF1 and a 68.9% downregulation in that of BK-β1. Transduction with Ad-GFP or Ad-scramble RNA served as controls (*n* = 9 culture plates). *C*: Adenoviral delivery of Nrf2 (50 MOI) enhanced the BK-β1 mRNA levels by 2.6-fold and 1.6-fold in cultured human and mouse coronary SMCs, respectively (*n* = 9 culture plates). *P* < 0.05 vs. controls. Ctrl, control.

expressions of Nrf2, HO-1, NF-κB/p65, MuRF1, and BK-β1 in cultured human coronary SMCs. A 12-h incubation with 10 μmol/L DMF produced a 1.9-fold and 1.6-fold augmentation, respectively, in Nrf2 and HO-1 protein expressions in human coronary SMCs, accompanied by a 43.9% and 63.8% reduction in NF-κB/p65 and MuRF1 expressions

and a threefold increase in BK-β1 protein levels (*n* = 6 culture plates for each group, *P* < 0.05 vs. controls) (Fig. 4*A*). Moreover, the BK-β1 mRNA expression was also upregulated by 15.3% in cells treated with DMF compared with cells treated with vehicle (*n* = 9 culture plates, *P* < 0.05) (Fig. 4*B*). These results indicate that the upregulation of
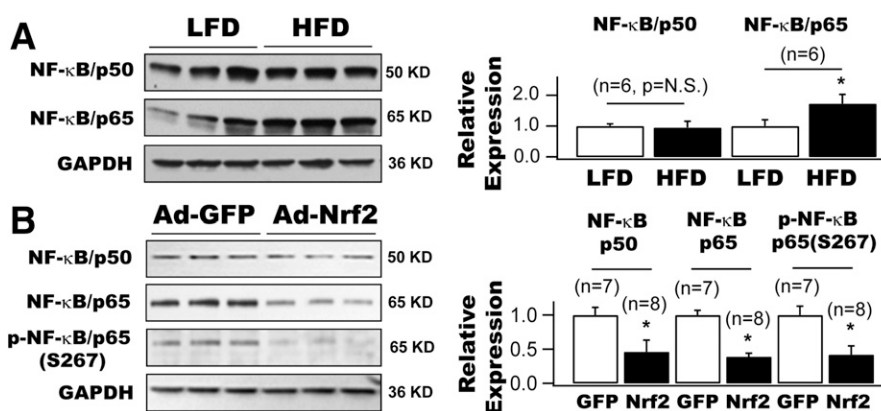
Figure 3—Regulation of NF-κB protein expressions by HFD and Nrf2 in primary human coronary arterial SMCs. *A*: Protein expressions of NF-κB/p50 and NF-κB/p65 were increased by 0.3-fold and 2.4-fold, respectively, in the arteries of HFD mice compared with those of LFD mice (*n* = 6 mice for each group). *B*: A 48-h transduction with Ad-Nrf2 suppressed the protein expressions of NF-κB/p50, NF-κB/p65, and phospho-NF-κB/p65(S267) in cultured human coronary arterial SMCs by 64.5%, 61.2%, and 58.0%, respectively (*n* = 7 to 8 culture plates). *P* < 0.05 vs. controls. p-NF-κB, phosphorylated NF-κB.
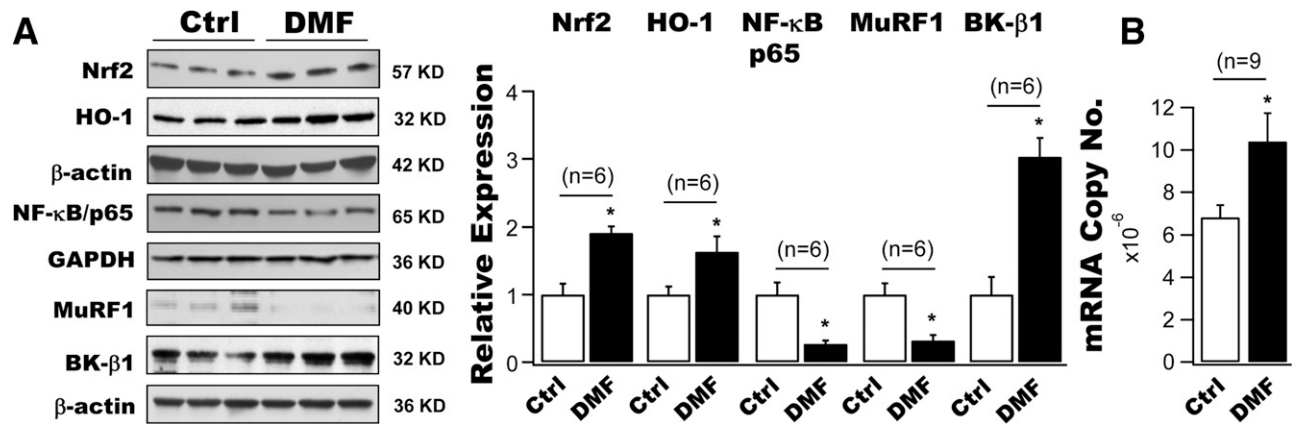
Figure 4—Effects of DMF on the protein expressions of Nrf2, HO-1, NK-κB, MuRF1, and BK-β1 in primary human coronary arterial SMCs in vitro. *A*: A 12-h incubation with 10 μmol/L DMF augmented the protein expressions of Nrf2 and HO-1 by 1.9-fold and 1.6-fold, respectively, accompanied by 43.9% and 63.8% reductions, respectively, in those of NF-κB/p65 and MuRF1 in cultured human coronary SMCs. These changes were associated with a threefold increase in BK-β1 protein levels in DMF-treated cells, compared with cells with vehicle treatment (*n* = 6 culture plates). *B*: A significant increase in BK-β1 mRNA expression by 15.3% in human coronary SMCs treated with DMF for 12 h compared with cells treated with vehicle (*n* = 9 culture plates for each group). *P* < 0.05 vs. controls. Ctrl, control.

BK-β1 protein expression by DMF is a result of increased mRNA transcription and attenuated protein degradation of BK-β1 in vascular SMCs.

Oral Administration of DMF Suppressed NF-κB/MuRF1-Dependent BK-β1 Protein Degradation in the Arteries of HFD Mice

We further investigated the effects of DMF in HFD mice in vivo. We found that a 10-day course of treatment with DMF by oral administration significantly reduced the body weight (51.1 ± 1.4 g with placebo vs. 38.6 ± 3.4 g with DMF, *n* = 10 for both groups, *P* < 0.05), and blood glucose levels (284.9 ± 16.0 mg/dL with placebo vs. 217.8 ± 17.9 mg/dL with DMF, *n* = 10 for both groups, *P* < 0.05) in HFD mice compared with those with placebo treatment. Interestingly, DMF had no significant effect on the body weights and blood glucose levels in LFD mice: 28.9 ± 0.6 g

with placebo vs. 28.7 ± 0.5 g with DMF (*n* = 9 for both groups, *P* = NS); and 168.1 ± 11.3 mg/dL with placebo vs. 150.7 ± 7.6 mg/dL with DMF (*n* = 9 for both groups, *P* = NS), respectively.

DMF treatment markedly enhanced the protein expressions of Nrf2 and BK-β1 in the arteries of HFD mice by 1.5-fold and 1.8-fold, respectively, whereas those of NF-κB/p50, NF-κB/p65, and MuRF1 were significantly downregulated by 56.8%, 75.5%, and 66.3% compared with HFD mice that received placebo treatment (*n* = 5 mice for each group, *P* < 0.05) (Fig. 5).

Oral Administration of DMF Protected Coronary BK Channel Function and BK Channel–Mediated Coronary Vasodilation in HFD Mice

Figure 6A shows the representative tracings and current-voltage curves of IBTX-sensitive K⁺ currents recorded from
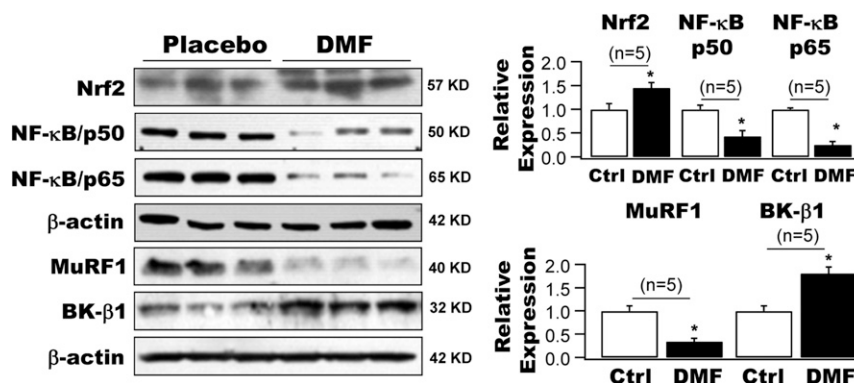
Figure 5—Effects of DMF on the protein expressions of Nrf2, NK-κB, MuRF1, and BK-β1 in HFD mouse arteries in vivo. A 10-day course of treatment with DMF by oral administration (25 mg/kg/daily) enhanced the protein expressions of Nrf2 and BK-β1 in the arteries of HFD mice by 1.5-fold and 1.8-fold, whereas it downregulated the protein expressions of NF-κB/p50, NF-κB/p65, and MuRF1 by 56.8%, 75.5%, and 66.3%, respectively, compared with HFD mice treated with placebo (*n* = 5 mice for each group). *P* < 0.05 vs. placebo. Ctrl, control.
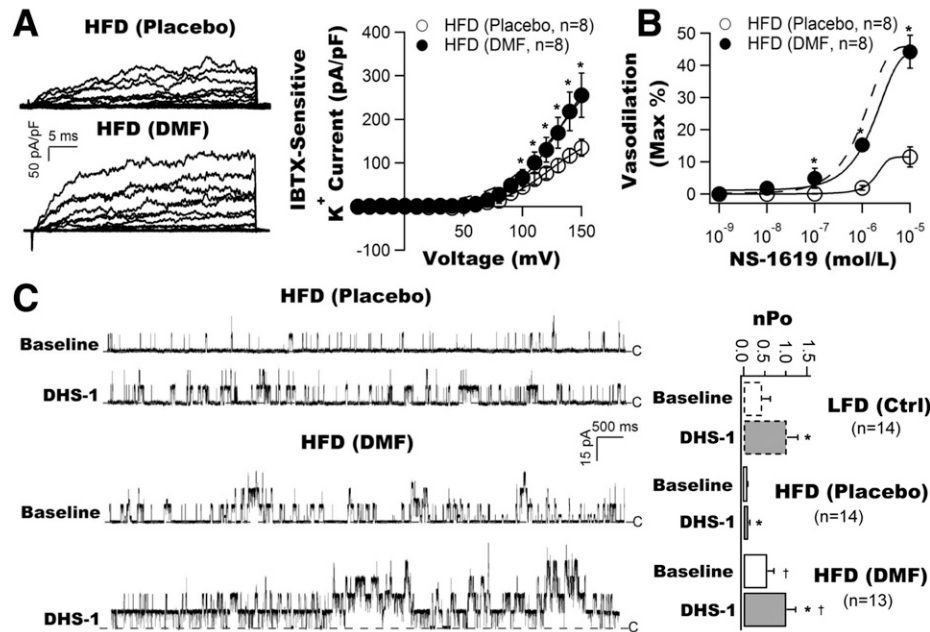
Figure 6—Protective effects of DMF administration on coronary BK channel current density, BK channel–mediated coronary vasodilation, and BK-β1–dependent activation in HFD mice. A: Representative tracings of whole-cell BK channel recordings and current voltage curves obtained from freshly isolated coronary SMCs of HFD mice after a 10-day course of treatment with DMF by gavage. Treatment with DMF restored the BK current density to a level comparable to that in LFD mice (dashed line) (n = 8 cells for each group). B: Treatment with DMF preserved NS-1619–mediated coronary vasodilation in HFD mice to a level similar to that in LFD mice (dashed line) (n = 8 mice for each group). C: Representative tracings of single-BK channel recordings in inside-out patches from freshly isolated coronary SMCs of HFD mice, elicited at 60 mV before and after exposure to DHS-1 (n = 13–14 cells). Animals were treated with DMF or placebo for 10 days, with DMF treatment preserving BK channel activity at baseline and restoring the channel response to DHS-1 in HFD mice to a level similar to that in LFD mice (open bar graphs). *P < 0.05 vs. baseline; †P < 0.05 vs. placebo. Ctrl, control.

freshly isolated coronary SMCs of HFD mice treated with DMF or placebo. BK current density was significantly increased in DMF-treated mice. It was 45.1 ± 8.4 pA/pF (n = 8 cells) with placebo and 73.1 ± 13.9 pA/pF with DMF (n = 8 cells, P < 0.05 vs. placebo) at 100 mV, which was similar to that in LFD mice without DMF treatment. Coronary vasodilation response to NS-1619 was impaired in placebo-treated HFD mice (n = 8), but it was preserved by DMF administration in HFD mice to a similar level to that in LFD control mice (n = 8) (Fig. 6B).

To further determine whether the protective effects of DMF on BK channel activities were mediated through BK-β1 function, we examined coronary BK channel activities in freshly isolated coronary SMCs in response to DHS-1 in HFD mice after a 10-day course of treatment with DMF by gavage. Figure 6C illustrates the single BK currents elicited at 60 mV from coronary SMCs of HFD mice treated with placebo or DMF. DMF treatment markedly increased the channel nPo at baseline compared with placebo treatment (0.09 ± 0.02 with placebo, n = 14 cells vs. 0.57 ± 0.15 with DMF, n = 14 cells, P < 0.001). Application of DHS-1 further enhanced the channel openings (nPo = 1.02 ± 0.21, n = 13, P < 0.001 vs. baseline of DMF-treated cells). In comparison, DHS-1 had no effects in placebo-treated cells (nPo = 0.10 ± 0.03, n = 13 cells, P = NS vs. baseline; P < 0.05 vs. DMF-treated cells). Importantly, BK channel

activities in HFD mice after DMF treatment were comparable to those in LFD mice before and after exposure to DHS-1. The nPo was 0.45 ± 0.18 at baseline in LFD cells (n = 14 cells, P = NS vs. the baseline of DMF-treated HFD cells) and 1.03 ± 0.18 after exposure to DHS-1 (n = 14 cells, P = NS vs. DMF-treated HFD cells with DHS-1). Hence, our results demonstrate that treatment with DMF restores coronary BK channel function and BK channel–mediated coronary vasoreactivity in HFD mice in vivo.

DISCUSSION

In this study, we found that a 6 months of consumption of an HFD increased mouse body weight and blood pressure, and serum glucose and insulin levels, which is consistent with previous reports (22–25). Since the average HbA_{1c} in patients with diabetes who have poor glycemic control in the U.S. is ~9% (32), corresponding to a blood glucose level of ~212 mg/dL, we believe that the HFD mice with a random average blood glucose level of 230 mg/dL is an excellent animal model for studying type 2 diabetes. We found that BK-β1 protein expression was significantly downregulated in HFD mouse arterial SMCs, resulting in impaired BK channel function. BK-β1 homeostasis is dependent on the balance between BK-β1 protein turnover and synthesis. It has been reported that decreased BK-β1 protein expression was associated with the nuclear factor

of activated T-cell c3 (NFATc3)–dependent inhibition of mRNA transcription in isolated mesentery arteries of HFD mice cultured with 20 mmol/L glucose for 48 h (13). In this study, we found that such a reduction of BK-β1 protein expression in coronary arteries of HFD mice was mainly due to accelerated proteolysis through the UPS because the BK-β1 mRNA levels were not altered in coronary arteries of HFD mice, which is similar to our findings in mice with streptozotocin-induced type 1 diabetes (9,11,16). The difference in findings might be due to the difference in experimental conditions and vessel bed specificity.

Nrf2 signaling is a master regulator of cellular redox status and detoxification responses (33,34). The function of Nrf2 is principally regulated by the Kelch-like ECH-associated protein 1 (Keap1), an adaptor protein for Cullin 3–dependent ubiquitination and degradation (35,36). Under normal conditions, Nrf2 is inhibited by binding to Keap1. Increase in oxidative stress or electrophile stimuli modifies specific cysteine residues in Keap1 and releases Nrf2 from binding with Keap1. The unbound Nrf2 translocates into the nucleus and heterodimerizes with small Maf proteins to form a transactivation machinery that binds to the promoter region of antioxidant response elements and electrophile response elements, which contain a Nrf2-binding motif [TGA(G/C)xxxGC] and/or a Maf-binding motif [TGCTGA

(G/C)] (37, 38). Clinical studies (39,40) have revealed that the reduction of Nrf2 expression contributes to oxidative stress in patients with chronic type 2 diabetes. One of our important findings in this study is that the regulation of vascular BK-β1 protein expression in HFD mice by Nrf2 was mediated through the NF-κB/MuRF1-dependent proteolysis. The protein expression of Nrf2 and BK-β1 was markedly decreased in HFD mice, whereas that of MuRF1 was increased. These reciprocal relationships were confirmed by manipulations of Nrf2 expression in cultured coronary arterial SMCs: adenoviral expression of Nrf2 gene profoundly upregulated the protein expression of BK-β1 and significantly downregulated that of MuRF1, whereas the knockdown of Nrf2 expression by Nrf2 shRNA had the opposite effects. However, the molecular mechanisms underlying Nrf2-regulating BK-β1 protein expression could be complicated. We found that Nrf2 overexpression also upregulated the BK-β1 mRNA expression in cultured coronary SMCs. It is not surprising since the KCNMB1 gene contains several consensus sequences of the Nrf2- and Maf-binding motifs in its promoter. Whether Nrf2 directly increases the KCNMB1 mRNA transcription or indirectly regulates other transcriptional factors that are responsible for BK-β1 transcription is currently unknown but warrants investigation. Nevertheless, an increase in BK-β1 mRNA expression and
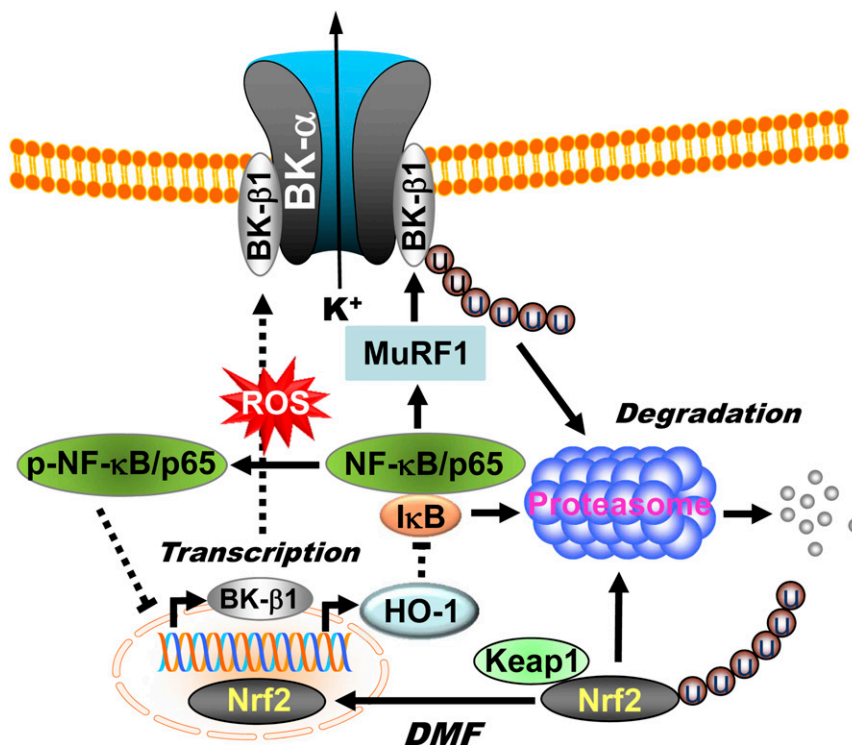
Figure 7—Illustration showing the role of Nrf2 signaling in the regulation of BK-β1 expression in arterial myocytes. Under normal conditions, Nrf2 is bound to Keap1, which promotes the degradation of Nrf2 through the UPS. Upon activation by DMF, Nrf2 dissociates from Keap1 and translocates into the nuclei, where the transcription of downstream effectors such as BK-β1 and HO-1 is facilitated. The metabolites of HO-1, such as CO, bilirubin, and Fe^{2+}, inhibit NF-κB activity. With increased oxidative stress in diabetic vessels, Nrf2 is downregulated, resulting in a reduction of BK-β1 and HO-1 expressions. In addition, increased ROS generation directly phosphorylates NF-κB/p65 at serine residues, which in turn promotes NF-κB/p65 nuclear translocation, facilitates MuRF1-dependent BK-β1 protein degradation, and suppresses Nrf2 transcriptional activity on BK-β1.

decrease in BK-β1 protein degradation by Nrf2 signaling would greatly modulate BK channel function in coronary SMCs.

The molecular mechanisms underlying the regulation of NF-κB expression by Nrf2 in diabetic vessels are currently unclear. It has been reported that the heme metabolites of HO-1, such as CO, bilirubin, and Fe^{2+}, are the core of Nrf2-mediated NF-κB inhibition (41–43). On the other hand, NF-κB/p65 deprives CREBPs from Nrf2, resulting in the suppression of Nrf2 transcriptional activity (44). In addition, the phosphorylation of serine residues in NF-κB/p65 could directly promote NF-κB/p65 nuclear translocation (15). The interplay between the Nrf2 and NF-κB pathways was confirmed by increased protein expression and transcriptional activity of NF-κB/p65 in the hearts of Nrf2 KO animals (45). In this study, we found that the protein expressions of NF-κB/p65 and were upregulated and those of Nrf2 and HO-1 were downregulated in the arteries of HFD mice. Such changes in protein profiles are favorable for MuRF1-dependent BK-β1 protein degradation in HFD mice. We believe that ROS plays an important role in the regulation of Nrf2 and NF-κB activity. Decrease of Nrf2 activity promotes ROS generation and facilitates NF-κB/p65 protein phosphorylation, which in turn attenuates the effects of Nrf2 on BK-β1 transcription and the NF-κB/MuRF1-dependent BK-β1 protein degradation. Adenoviral expression of Nrf2 gene enhanced HO-1 protein expression and reduced NF-κB/p50 and NF-κB/p65 and phospho-NF-κB/p65(S267) protein expressions in human coronary SMCs. The scheme illustrating the role of Nrf2 signaling in the regulation of vascular BK-β1 expression is shown in Fig. 7.

It has been reported that DMF enhances Nrf2 transcriptional activity through covalently binding to the reactive cysteine residues of Keap1, thereby preventing the proteolytic degradation of Nrf2 in the UPS (46). Recently, DMF (Tecfidera) has been successfully used in the treatment of human relapsing multiple sclerosis with no major adverse events (47,48) but has not been applied to the treatment of diabetic vascular complications. We show that the treatment of human coronary SMCs and HFD mouse coronary arteries with this Food and Drug Administration–approved drug suppressed the NF-κB/MuRF1-induced BK-β1 protein degradation and enhanced BK-β1 mRNA transcription, in turn protecting coronary BK channel function and BK channel–mediated coronary vasodilation in HFD mice. Moreover, a 10-day course of treatment with DMF by oral administration resulted in significantly decreased body weights and serum glucose levels in HFD mice, whereas DMF had no such effects in LFD mice. These novel results provide the first evidence that Nrf2 activation is an exciting strategy for the treatment of BK channelopathy and vasculopathy in obese/diabetic animals.

References

1. Nelson MT, Cheng H, Rubart M, et al. Relaxation of arterial smooth muscle by calcium sparks. Science 1995;270:633–637
2. Ledoux J, Werner ME, Brayden JE, Nelson MT. Calcium-activated potassium channels and the regulation of vascular tone. Physiology (Bethesda) 2006;21:69–78
3. Krishnamoorthy-Natarajan G, Koide M. BK Channels in the Vascular System. Int Rev Neurobiol 2016;128:401–438
4. Lu T, Jiang B, Wang XL, Lee HC. Coronary arterial BK channel dysfunction exacerbates ischemia/reperfusion-induced myocardial injury in diabetic mice. Appl Physiol Nutr Metab 2016;41:992–1001
5. McManus OB, Helms LM, Pallanck L, Ganetzky B, Swanson R, Leonard RJ. Functional role of the beta subunit of high conductance calcium-activated potassium channels. Neuron 1995;14:645–650
6. Meera P, Wallner M, Jiang Z, Toro L. A calcium switch for the functional coupling between alpha (hslo) and beta subunits (Kv,cabeta) of maxi K channels. FEBS Lett 1996;385:127–128
7. Cox DH, Aldrich RW. Role of the beta1 subunit in large-conductance $Ca^{(2+)}$-activated $K^{(+)}$ channel gating energetics. Mechanisms of enhanced $Ca^{(2+)}$ sensitivity. J Gen Physiol 2000;116:411–432
8. McGahon MK, Dash DP, Arora A, et al. Diabetes downregulates large-conductance Ca^{2+}-activated potassium beta 1 channel subunit in retinal arteriolar smooth muscle. Circ Res 2007;100:703–711
9. Zhang DM, He T, Katusic ZS, Lee HC, Lu T. Muscle-specific f-box only proteins facilitate bk channel β(1) subunit downregulation in vascular smooth muscle cells of diabetes mellitus. Circ Res 2010;107:1454–1459
10. Wang RX, Shi HF, Chai Q, et al. Molecular mechanisms of diabetic coronary dysfunction due to large conductance $Ca2^+$-activated K^+ channel impairment. Chin Med J (Engl) 2012;125:2548–2555
11. Lu T, Chai Q, Yu L, et al. Reactive oxygen species signaling facilitates FOXO-3a/FBXO-dependent vascular BK channel β1 subunit degradation in diabetic mice. Diabetes 2012;61:1860–1868
12. Rueda A, Fernández-Velasco M, Benitah JP, Gómez AM. Abnormal Ca^{2+} spark/STOC coupling in cerebral artery smooth muscle cells of obese type 2 diabetic mice. PLoS One 2013;8:e53321
13. Nystoriak MA, Nieves-Cintrón M, Nygren PJ, et al. AKAP150 contributes to enhanced vascular tone by facilitating large-conductance Ca^{2+}-activated K^+ channel remodeling in hyperglycemia and diabetes mellitus. Circ Res 2014;114:607–615
14. Hayden MS, Ghosh S. Signaling to NF-kappaB. Genes Dev 2004;18:2195–2224
15. Narayanan A, Amaya M, Voss K, et al. Reactive oxygen species activate NFκB (p65) and p53 and induce apoptosis in RVFV infected liver cells. Virology 2014;449:270–286

16. Yi F, Wang H, Chai Q, et al. Regulation of large conductance Ca2+-activated K+ (BK) channel β1 subunit expression by muscle RING finger protein 1 in diabetic vessels. J Biol Chem 2014;289:10853–10864

17. Chen J, Zhang Z, Cai L. Diabetic cardiomyopathy and its prevention by nrf2: current status. Diabetes Metab J 2014;38:337–345

18. Gao L, Mann GE. Vascular NAD(P)H oxidase activation in diabetes: a double-edged sword in redox signalling. Cardiovasc Res 2009;82:9–20

19. Nguyen T, Nioi P, Pickett CB. The Nrf2-antioxidant response element signaling pathway and its activation by oxidative stress. J Biol Chem 2009;284:13291–13295

20. Taguchi K, Motohashi H, Yamamoto M. Molecular mechanisms of the Keap1–Nrf2 pathway in stress response and cancer evolution. Genes Cells 2011;16:123–140

21. Li B, Liu S, Miao L, Cai L. Prevention of diabetic complications by activation of Nrf2: diabetic cardiomyopathy and nephropathy. Exp Diabetes Res 2012;2012:216512

22. Winzell MS, Ahrén B. The high-fat diet-fed mouse: a model for studying mechanisms and treatment of impaired glucose tolerance and type 2 diabetes. Diabetes 2004;53(Suppl. 3):S215–S219

23. Alexander J, Chang GQ, Dourmashkin JT, Leibowitz SF. Distinct phenotypes of obesity-prone AKR/J, DBA2J and C57BL/6J mice compared to control strains. Int J Obes 2006;30:50–59

24. Collins S, Martin TL, Surwit RS, Robidoux J. Genetic vulnerability to diet-induced obesity in the C57BL/6J mouse: physiological and molecular characteristics. Physiol Behav 2004;81:243–248

25. Petro AE, Cotter J, Cooper DA, Peters JC, Surwit SJ, Surwit RS. Fat, carbohydrate, and calories in the development of diabetes and obesity in the C57BL/6J mouse. Metabolism 2004;53:454–457

26. Considine RV, Considine EL, Williams CJ, et al. Mutation screening and identification of a sequence variation in the human ob gene coding region. Biochem Biophys Res Commun 1996;220:735–739

27. King AJ. The use of animal models in diabetes research. Br J Pharmacol 2012;166:877–894

28. Jing X, Shi H, Zhang C, et al. Dimethyl fumarate attenuates 6-OHDA-induced neurotoxicity in SH-SY5Y cells and in animal model of Parkinson's disease by enhancing Nrf2 activity. Neuroscience 2015;286:131–140

29. Oh CJ, Kim JY, Choi YK, et al. Dimethylfumarate attenuates renal fibrosis via NF-E2-related factor 2-mediated inhibition of transforming growth factor-β/Smad signaling. PLoS One 2012;7:e45870

30. Lu T, Ye D, He T, Wang XL, Wang HL, Lee HC. Impaired Ca^{2+}-dependent activation of large-conductance Ca^{2+}-activated K$^+$ channels in the coronary artery smooth muscle cells of Zucker Diabetic Fatty rats. Biophys J 2008;95:5165–5177

31. Lu T, Zhang DM, Wang XL, et al. Regulation of coronary arterial BK channels by caveolae-mediated angiotensin II signaling in diabetes mellitus. Circ Res 2010;106:1164–1173

32. Ali MK, McKeever Bullard K, Imperatore G, Barker L, Gregg EW; Centers for Disease Control and Prevention (CDC). Characteristics associated with poor glycemic control among adults with self-reported diagnosed diabetes—National Health and Nutrition Examination Survey, United States, 2007-2010. MMWR Suppl 2012;61:32–37

33. Ma Q. Role of nrf2 in oxidative stress and toxicity. Annu Rev Pharmacol Toxicol 2013;53:401–426

34. Suzuki T, Yamamoto M. Molecular basis of the Keap1-Nrf2 system. Free Radic Biol Med 2015;88(Pt B):93–100

35. Canning P, Sorrell FJ, Bullock AN. Structural basis of Keap1 interactions with Nrf2. Free Radic Biol Med 2015;88:101–107

36. Kobayashi A, Kang MI, Okawa H, et al. Oxidative stress sensor Keap1 functions as an adaptor for Cul3-based E3 ligase to regulate proteasomal degradation of Nrf2. Mol Cell Biol 2004;24:7130–7139

37. Chorley BN, Campbell MR, Wang X, et al. Identification of novel NRF2-regulated genes by ChIP-Seq: influence on retinoid X receptor alpha. Nucleic Acids Res 2012;40:7416–7429

38. Yoshida T, Ohkumo T, Ishibashi S, Yasuda K. The 5'-AT-rich half-site of Maf recognition element: a functional target for bZIP transcription factor Maf. Nucleic Acids Res 2005;33:3465–3478

39. Jiménez-Osorio AS, Picazo A, González-Reyes S, Barrera-Oviedo D, Rodríguez-Arellano ME, Pedraza-Chaverri J. Nrf2 and redox status in prediabetic and diabetic patients. Int J Mol Sci 2014;15:20290–20305

40. Santillán LD, Moyano M, Frau M, et al. Reduced blood nrf-2 mRNA in local overweight boys at risk of metabolic complications: a study in San Luis City, San Luis, Argentina. Metab Syndr Relat Disord 2013;11:359–365

41. Soares MP, Seldon MP, Gregoire IP, et al. Heme oxygenase-1 modulates the expression of adhesion molecules associated with endothelial cell activation. J Immunol 2004;172:3553–3563

42. Bellezza I, Tucci A, Galli F, et al. Inhibition of NF-κB nuclear translocation via HO-1 activation underlies α-tocopheryl succinate toxicity. J Nutr Biochem 2012;23:1583–1591

43. Brunt KR, Tsuji MR, Lai JH, et al. Heme oxygenase-1 inhibits pro-oxidant induced hypertrophy in HL-1 cardiomyocytes. Exp Biol Med (Maywood) 2009;234:582–594

44. Liu Y, Sellke EW, Feng J, et al. Calcium-activated potassium channels contribute to human skeletal muscle microvascular endothelial dysfunction related to cardiopulmonary bypass. Surgery 2008;144:239–244

45. Al-Sawaf O, Fragoulis A, Rosen C, et al. Nrf2 protects against TWEAK-mediated skeletal muscle wasting. Sci Rep 2014;4:3625

46. Takaya K, Suzuki T, Motohashi H, et al. Validation of the multiple sensor mechanism of the Keap1-Nrf2 system. Free Radic Biol Med 2012;53:817–827

47. Fox RJ, Miller DH, Phillips JT, et al.; CONFIRM Study Investigators. Placebo-controlled phase 3 study of oral BG-12 or glatiramer in multiple sclerosis. N Engl J Med 2012;367:1087–1097

48. Hutchinson M, Fox RJ, Miller DH, et al. Clinical efficacy of BG-12 (dimethyl fumarate) in patients with relapsing-remitting multiple sclerosis: subgroup analyses of the CONFIRM study. J Neurol 2013;260:2286–2296